

# Bags, junctions, and networks of BPS and non-BPS defects

D. Bazeia and F.A. Brito

*Departamento de Física, Universidade Federal da Paraíba,  
Caixa Postal 5008, 58051-970 João Pessoa, Paraíba, Brazil*

(August 14, 2018)

We investigate several models of coupled scalar fields that present discrete  $Z_2$ ,  $Z_2 \times Z_2$ ,  $Z_3$  and other symmetries. These models support topological domain wall solutions of the BPS and non-BPS type. The BPS solutions are stable, but the stability of the non-BPS solutions may depend on the parameters that specify the models. The BPS and non-BPS states give rise to bags, and also to three-junctions that may allow the presence of networks of topological defects. In particular, we show that the non-BPS defects of a specific model that engenders the  $Z_3$  symmetry give rise to a stable regular hexagonal network of domain walls.

PACS numbers: 11.27.+d, 11.30.Er, 11.30.Pb

## I. INTRODUCTION

Bogomol'nyi, and Prasad and Sommerfield [1], have presented a way to find topological solutions that saturate the lower bound in energy. These solutions are known as BPS states, and they are supposed to play some role in the development of modern particle physics, because there are supersymmetric models where they are shorter multiplets, stable, and no continuum variation of parameters can modify these BPS states. In Refs. [2–4] one has investigated some models of coupled real scalar fields in bidimensional space-time. These models present peculiar features, such as the presence of the Bogomol'nyi bound, with the corresponding appearance of first-order differential equations that solve the equations of motion in the case of static configurations. These Refs. [2–4] have found topological solitons in specific models by taking advantage of the trial-orbit method first introduced by Rajaraman in Ref. [5]. These investigations provide a concrete way of finding BPS states and suggest several other studies, in particular on the subject of defects inside defects, as presented for instance in Refs. [6–8] and more recently in [9–15]. The investigations of defects inside defects presented in Ref. [11,12,14,15] are natural extensions of the former papers [2–4].

In supersymmetric models with chiral superfields the presence of discrete symmetry may produce BPS and non-BPS walls. The non-BPS walls are solutions of the equations of motion, and they do not necessarily saturate the lower bound in energy. But the BPS walls saturate the lower bound in energy, and lie in shorter multiplets, in a way such that they preserve the supersymmetry only partially [16–18]. There are BPS states that preserve 1/2 and 1/4 of the supersymmetry [16–23], and in the present work we investigate several explicit examples. We start by first offering general considerations in Sec. II. We examine specific models in Sec. III, where we find several solutions, of the BPS and non-BPS type. See also the more recent work [25,26], where one can find other inves-

tigations concerning the BPS domain wall junctions in supersymmetric models.

Our work continues in Sec. IV, where we investigate stability of several BPS and non-BPS solutions. This is done not only to show stability, but also to see how the bosonic matter behaves in the background of BPS and non-BPS defects. The behavior of the fermionic matter in the extended supersymmetric models can be investigated by following the lines of Refs. [14,27,28]. In Sec. V we investigate two other issues. The first in Sec. V A, where we consider the entrapment of the other field, as in bag models [29–31]. This possibility may be implemented in the first, second and third models, and the bag may be of the BPS or non-BPS type, depending of the particular model under consideration. We examine the second issue in Sec. V B, where we investigate fusion of defects. Here we briefly review Ref. [20], which introduces investigations valid within the supersymmetric context, and after we offer another possibility of showing fusion of defects and stability of junctions, valid beyond the context of supersymmetry.

In Sec. VI we show how one can generate planar networks of BPS and non-BPS defects. There we show that the three-junction that appears in supersymmetric models may be stable, but cannot generate a BPS network of defects. However, when we give up supersymmetry we find a model where domain wall junctions are stable, the three-junction strictly obey the triangle inequality and generate a stable network of defects. We summarize the main results in Sec. VII, where we end the present work.

The subject of this work may find direct applications in diverse branches of physics. Besides the recent interest, put forward in Refs. [21–23], we recall for instance that the  $Z_3$  group is the center of  $SU(3)$ , and this may guide us toward applications involving strong interactions. Some examples can be found in Ref. [32,33]. Another possibility is related to the  $Z_2 \times Z_3$  symmetry, in an effort to entrap the  $Z_3$ -symmetric portion of the model inside the topological defect generated by the  $Z_2$  symmetry.

Other applications include issues related to cosmology [34] and magnetic materials [35], and to pattern formation in systems of condensed matter [36]. The investigations that we present are done in flat space-time, in the  $(d, 1)$  dimensional case. We use natural units, taking  $\hbar = c = 1$ , and the metric tensor presents signature in the form  $(+, -, \dots, -)$ . In the present work we are mainly concerned with the cases  $d = 1, 2$ , and  $3$ . We specify the spatial dimension along with the interest of the subject under investigation.

## II. GENERAL CONSIDERATIONS

Let us start with two real scalar fields  $\phi$  and  $\chi$ . We consider models defined via the Lagrangian density

$$\mathcal{L} = \frac{1}{2} \partial_\alpha \phi \partial^\alpha \phi + \frac{1}{2} \partial_\alpha \chi \partial^\alpha \chi - V \quad (1)$$

This is valid in  $(d, 1)$  space-time dimensions.  $V = V(\phi, \chi)$  is the potential. It has the general form

$$V(\phi, \chi) = \frac{1}{2} W_\phi^2 + \frac{1}{2} W_\chi^2 \quad (2)$$

$W = W(\phi, \chi)$  is some smooth function of the fields  $\phi$  and  $\chi$ , and  $W_\phi = (\partial W / \partial \phi)$  etc. This is the form of the (real bosonic portions of the) models we deal with in the present work. These models admit a supersymmetric extension, and in the supersymmetric theory the function  $W$  is the superpotential.

Models defined via  $W(\phi, \chi)$  present several interesting properties [2–4]. The equations of motion are

$$\frac{\partial^2 \phi}{\partial t^2} - \nabla^2 \phi + \frac{\partial V}{\partial \phi} = 0 \quad (3)$$

$$\frac{\partial^2 \chi}{\partial t^2} - \nabla^2 \chi + \frac{\partial V}{\partial \chi} = 0 \quad (4)$$

For static field configurations living in the  $(1, 1)$  space-time, that is, for fields  $\phi = \phi(x)$  and  $\chi = \chi(x)$  they reduce to

$$\frac{d^2 \phi}{dx^2} = W_\phi W_{\phi\phi} + W_\chi W_{\chi\phi} \quad (5)$$

$$\frac{d^2 \chi}{dx^2} = W_\phi W_{\phi\chi} + W_\chi W_{\chi\chi} \quad (6)$$

These equations are solved by first-order differential equations

$$\frac{d\phi}{dx} = W_\phi \quad (7)$$

$$\frac{d\chi}{dx} = W_\chi \quad (8)$$

The energy of solutions that solve the first-order equations are bounded to the value  $E_B^{ij} = |\Delta W_{ij}|$ , where

$$\Delta W_{ij} = W(\phi_i, \chi_i) - W(\phi_j, \chi_j) \quad (9)$$

Here  $(\phi_i, \chi_i)$  is the  $i$ -th vacuum state of the model under consideration. The reason for this is simple: the energy of static configurations is

$$E = \frac{1}{2} \int_{-\infty}^{\infty} dx \left[ \left( \frac{d\phi}{dx} \right)^2 + \left( \frac{d\chi}{dx} \right)^2 + W_\phi^2 + W_\chi^2 \right] \quad (10)$$

It can be rewritten in the form

$$E = \frac{1}{2} \int_{-\infty}^{\infty} dx \left[ \left( \frac{d\phi}{dx} - W_\phi \right)^2 + \left( \frac{d\chi}{dx} - W_\chi \right)^2 \right] + \int_{-\infty}^{\infty} dx \left( W_\phi \frac{d\phi}{dx} + W_\chi \frac{d\chi}{dx} \right) \quad (11)$$

We recall that

$$\frac{dW}{dx} = W_\phi \frac{d\phi}{dx} + W_\chi \frac{d\chi}{dx} \quad (12)$$

to see that the energy gets to the bound  $E_B$  when the field configurations obey the first-order equations (7) and (8). This is the Bogomol'nyi bound, and the corresponding solutions are BPS solutions. The BPS solutions are linearly or classically stable – see Sec. IV.

The energy of BPS solutions can be also written as

$$E_B = \int_{-\infty}^{\infty} dx \left[ \left( \frac{d\phi}{dx} \right)^2 + \left( \frac{d\chi}{dx} \right)^2 \right] \quad (13)$$

$$= \int_{-\infty}^{\infty} dx (W_\phi^2 + W_\chi^2) \quad (14)$$

The above result shows that the gradient (g) and potential (p) portions of the energy

$$g = \int_{-\infty}^{\infty} dx g(x) = \int_{-\infty}^{\infty} dx \frac{1}{2} \left[ \left( \frac{d\phi}{dx} \right)^2 + \left( \frac{d\chi}{dx} \right)^2 \right] \quad (15)$$

$$p = \int_{-\infty}^{\infty} dx p(x) = \int_{-\infty}^{\infty} dx \frac{1}{2} (W_\phi^2 + W_\chi^2) \quad (16)$$

contribute evenly to the total energy of the solution. Although this is shared by all the BPS states, it is not peculiar to BPS states, since there are non-BPS states that also have energy evenly distributed in its potential and gradient portions – see below.

In the case of two scalar fields, there are other possible arrangements to the energy (10). We can, for instance, consider the possibility

$$E = \frac{1}{2} \int_{-\infty}^{\infty} dx \left[ \left( \frac{d\phi}{dx} - W_\chi \right)^2 + \left( \frac{d\chi}{dx} - W_\phi \right)^2 \right] + \int_{-\infty}^{\infty} dx \left( W_\phi \frac{d\chi}{dx} + W_\chi \frac{d\phi}{dx} \right) \quad (17)$$

This expression is also minimized to obey Eqs. (13) and (14) when one sets

$$\frac{d\phi}{dx} = W_\chi \quad (18)$$

$$\frac{d\chi}{dx} = W_\phi \quad (19)$$

We can show that solutions to these equations (18) and (19) only solve the equations of motion when we impose on  $W(\phi, \chi)$  the extra condition

$$W_{\phi\phi} = W_{\chi\chi} \quad (20)$$

Unfortunately, however, this condition (20) factorizes  $W(\phi, \chi)$  into the sum  $W_+(\phi_+) + W_-(\phi_-)$  when one rotates the  $(\phi, \chi)$  plane to  $(\phi_+, \phi_-)$ , with

$$\phi_\pm = \frac{1}{\sqrt{2}}(\chi \pm \phi) \quad (21)$$

as firstly shown in Ref. [15]. The condition (20) turns the system into two decoupled systems.

We can consider another possibility to rewrite the energy (10). We set

$$E = \frac{1}{2} \int_{-\infty}^{\infty} dx \left[ \left( \frac{d\phi}{dx} + W_\chi \right)^2 + \left( \frac{d\chi}{dx} - W_\phi \right)^2 \right] + \int_{-\infty}^{\infty} dx \left( W_\phi \frac{d\chi}{dx} - W_\chi \frac{d\phi}{dx} \right) \quad (22)$$

This expression is also minimized to obey (13) and (14) when we write

$$\frac{d\phi}{dx} = -W_\chi \quad (23)$$

$$\frac{d\chi}{dx} = W_\phi \quad (24)$$

These equations (23) and (24) solve the equations of motion when one imposes on  $W(\phi, \chi)$  the extra condition

$$W_{\phi\phi} + W_{\chi\chi} = 0 \quad (25)$$

This result is interesting. It shows that for  $W(\phi, \chi)$  harmonic, we can solve the two (second-order differential) equations of motion (5) and (6) with two sets of two first-order differential equations, the set of Bogomol'nyi equations (7) and (8), and another one, given by Eqs. (23) and (24).

We make good use of this result by imposing that the second set of first-order equations (23) and (24) are still Bogomol'nyi equations, that appear via the presence of another function  $\widetilde{W}$ . This new function is defined by

$$\widetilde{W}_\phi = -W_\chi \quad (26)$$

$$\widetilde{W}_\chi = W_\phi \quad (27)$$

Since  $W$  and  $\widetilde{W}$  are smooth functions, they are necessarily harmonic. We then get the result that potentials defined by harmonic functions can always be written in

terms of two functions,  $W$  and  $\widetilde{W}$ . We use this to introduce the complex superpotential

$$\mathcal{W} = W + i\widetilde{W} \quad (28)$$

The superpotential  $\mathcal{W} = \mathcal{W}(\varphi)$  now depends on the complex field  $\varphi = \phi + i\chi$ , and the harmonicity of both  $W$  and  $\widetilde{W}$  appears via the Cauchy condition on  $\mathcal{W}$ . This is the way we get from the investigations [2–4] to the recent work in Refs. [21–23].

We guide ourselves toward the topological solutions by introducing a topological current. This is the standard procedure, and we can introduce for instance the topological current

$$J_{BPS}^\alpha = \varepsilon^{\alpha\beta} \partial_\beta \mathcal{W}(\phi, \chi) \quad (29)$$

It is defined in terms of  $\mathcal{W}(\phi, \chi)$ , and the topological charge is directly identified with the energy of the topological solution that satisfies the pair of first-order equations (7) and (8). This definition identifies the topological charge with the energy of the BPS solution. It expresses the fact that the mass of a BPS state is completely determined by its topological charge. This definition provides a single way to infer stability of the BPS states. This is a nice way of defining the topological current, but it is not complete, because it cannot see sectors of the non-BPS type. It is only effective for BPS sectors, and that is the reason for the label BPS assigned to it. However, since we need to identify every topological sector, we should use another topological current. We can consider, for instance

$$J^\alpha = \varepsilon^{\alpha\beta} \partial_\beta \begin{pmatrix} \phi \\ \chi \end{pmatrix} \quad (30)$$

It obeys  $\partial_\alpha J^\alpha = 0$ , and it is also a vector in the  $(\phi, \chi)$  plane. The topological current (30) is the current that we shall use in this work. We use this definition to obtain, for static configurations

$$J_\alpha^t J^\alpha = \rho^t \rho = 2g(x) \quad (31)$$

where  $g(x)$  is the gradient energy density of the solution. This property can be used to infer stability of junctions, for configurations that present energy density evenly distributed in their gradient and potential energy densities. This is so because in this case  $\rho^t \rho = 2g(x) = g(x) + p(x)$  gives the full energy density, and may be used to show that the junction process occurs exothermically. This result was already introduced in Ref. [24], and offers a way of showing how the process of junctions of defects may occur exothermically in models defined outside the context of supersymmetry – see Sec. V B.

Up to here the calculations were done in (1, 1) space-time dimensions. However, we can easily immerse the system into (2, 1) or into (3, 1) space-time dimensions. In the first case, in  $d = 2$  the solutions can be seen as domain ribbons, and the energy is now multiplied by the

length of the ribbons. In the second case, in  $d = 3$  we get domain walls, and the energy is to be multiplied by the area of the wall. The planar case is necessary for introducing junctions of domain ribbons [or of domain walls if one immerses the system in the  $(3, 1)$  space-time] and their corresponding planar networks. There are several distinct possibilities, and in the sequel we specify some cases. We recall that we single out topological sectors using pairs of vacuum states. For BPS sectors the energy is obtained via the superpotential, and we shall also use the notation  $t_{ij} = |W(\phi_i, \chi_i) - W(\phi_j, \chi_j)|$ , identifying the BPS sectors with tensions or energies of the topological defects.

### III. SOME SPECIFIC MODELS

Our aim here is to introduce models of coupled scalar fields, to illustrate how one can find topological solutions of the BPS and non-BPS type. We investigate several models of coupled scalar fields, defined with smooth functions  $W(\phi, \chi)$ . We organize the subject in the four subsections that follow, where we examine four different models.

#### A. The first model

We consider the superpotential

$$W^{(1)}(\phi, \chi) = -\lambda\phi + \frac{1}{3}\lambda\phi^3 + \mu\phi\chi^2 \quad (32)$$

where  $\lambda$  and  $\mu$  are real parameters. This model was first investigated in Ref. [2], but here we bring new results. The equations of motion for static field configurations are given by

$$\frac{d^2\phi}{dx^2} = 2\lambda^2\phi(\phi^2 - 1) + 2\mu^2(2 + \frac{\lambda}{\mu})\phi\chi^2 \quad (33)$$

$$\frac{d^2\chi}{dx^2} = 2\lambda\mu(\phi^2 - 1)\chi + 4\mu^2\phi^2\chi + 2\mu^2\chi^3 \quad (34)$$

These equations are solved by configurations that also solve the pair of first-order differential equations

$$\frac{d\phi}{dx} = \lambda(\phi^2 - 1) + \mu\chi^2 \quad (35)$$

$$\frac{d\chi}{dx} = 2\mu\phi\chi \quad (36)$$

Solutions that solve these first-order equations are BPS solutions.

This model has four absolute minima when  $\lambda/\mu > 0$ , and two minima when  $\lambda/\mu < 0$ . For  $\lambda/\mu > 0$  the minima are  $(\pm 1, 0)$  and  $(0, \pm\sqrt{\lambda/\mu})$ . Topological solutions are solutions that connect adjacent minima. Thus, the asymptotic behavior of the fields is governed by the set

of minima of the potential. For  $\lambda/\mu > 0$  the system supports several topological sectors. Their energies or tensions are given by, for solutions that connect the minima  $(-1, 0)$  and  $(1, 0)$

$$t_{BPS}^1 = \frac{4}{3}|\lambda| \quad (37)$$

For solutions that connect the minima  $(\pm 1, 0)$  and  $(0, \pm\sqrt{\lambda/\mu})$  we get

$$\bar{t}_{BPS}^1 = \frac{2}{3}|\lambda| \quad (38)$$

For the non-BPS solution that connects the minima  $(0, \sqrt{\lambda/\mu})$  and  $(0, -\sqrt{\lambda/\mu})$  we obtain

$$t_{nBPS}^1 = \frac{4}{3}|\lambda| \sqrt{\frac{\lambda}{\mu}} \quad (39)$$

There are BPS solutions in the first sector, which connects the two minima  $(\pm 1, 0)$ . They are

$$\phi(x) = -\tanh(\lambda x) \quad (40)$$

$$\chi(x) = 0 \quad (41)$$

and

$$\phi(x) = -\tanh(2\mu x) \quad (42)$$

$$\chi(x) = \pm \sqrt{\frac{\lambda}{\mu} - 2} \operatorname{sech}(2\mu x) \quad (43)$$

The first pair is of the one-component type, and is important for investigating the presence of defects inside defects – see for instance Refs. [11,12,14,15]. The second pair is of the two-component type, and may play a role in applications to condensed matter, as for instance in the case investigated in Refs. [4,37].

The one-component and the two-component type of solutions also appear in magnetic materials [35]. There they are known as Ising and Bloch walls, respectively. The two-component Bloch wall has a peculiar behavior, that can be used to understand specific features of interfaces between magnetic domains. The issue here is that if one looks at these solutions as vectors in the  $(\phi, \chi)$  plane, for  $x$  spanning the interval  $(-\infty, \infty)$  they describe a straight line and an elliptical arc connection between the two minima  $(\pm 1, 0)$ , respectively, behaving very much like linearly and elliptically polarized light. For this reason, the Bloch walls can be seen as chiral interfaces between domains with different magnetization, and this can be used to describe the wall motion in magnetic materials [38]. Furthermore, these walls can be charged and we may introduce charge by making the  $\chi$  field complex, or by coupling fermions to the system.

For  $\lambda/\mu < 0$  we have only two vacuum states. They are  $(\pm 1, 0)$  and now we have a single topological sector, with the same energy and topological charge obtained before,

for the corresponding sector. We notice that the first pair of solutions (40) and (41) solves the first-order equations even for  $\lambda/\mu < 0$ . This one-component solution is still of the BPS type for  $\lambda/\mu < 0$ , but now no topological defect can be nested inside it. The reason is that for  $\lambda/\mu < 0$  the model presents no spontaneous symmetry breaking in the independent  $\chi$  direction, and so it cannot support topological defect in this  $\chi$  direction anymore.

For  $\lambda/\mu > 0$ , there are non-BPS solutions connecting  $(0, \sqrt{\lambda/\mu})$  and  $(0, -\sqrt{\lambda/\mu})$  by a straight line. To see this explicitly we consider  $\phi = 0$  in the specific system to get the equation of motion for the static field  $\chi = \chi(x)$

$$\frac{d^2\chi}{dx^2} = 2\mu^2 \left( \chi^2 - \frac{\lambda}{\mu} \right) \chi \quad (44)$$

The solutions are

$$\chi(x) = \pm \sqrt{\frac{\lambda}{\mu}} \tanh(\sqrt{\lambda\mu} x) \quad (45)$$

The corresponding non-BPS energy is  $(4/3)|\lambda| \sqrt{\lambda/\mu}$ , as already presented in Eq. (39).

This model decouples for  $\lambda = \mu$ , as we have already shown in Ref. [12]. In this case the symmetry  $Z_2 \times Z_2$  changes to the  $Z_4$  one, but here a rotation by  $\pi/4$  changes the model into two single-field models. We also note that for  $\lambda = -2\mu$ , the model decouples into two single-field systems, showing that the limit  $\mu \rightarrow -\lambda/2$  is also uninteresting, at least from the point of view of models of coupled scalar field.

We expose other features of the model using  $W^{(1)}$ . We write

$$W_{\phi\phi}^{(1)} = 2\lambda\phi, \quad W_{\chi\chi}^{(1)} = 2\mu\phi, \quad W_{\phi\chi}^{(1)} = 2\mu\chi \quad (46)$$

We see that  $W^{(1)}$  is harmonic when  $\mu \rightarrow -\lambda$ . This means that the model admits another pair of first-order equations. This pair follows from (23) and (24)

$$\frac{d\phi}{dx} = 2\mu\phi\chi \quad (47)$$

$$\frac{d\chi}{dx} = \lambda - \lambda\phi^2 - \mu\chi^2 \quad (48)$$

These equations also furnish solutions to the equations of motion, for  $\mu \rightarrow -\lambda$ . As we have already seen, for  $\mu \rightarrow -\lambda$  the model presents a single topological sector, already investigated. But we notice that  $W^{(1)}$  is also harmonic in the limit  $\phi \rightarrow 0$ , independently of the parameters  $\lambda$  and  $\mu$ . We use this into the above Eqs. (47) and (48) to get  $\phi = 0$  and

$$\frac{d\chi}{dx} = -\mu \left( \chi^2 - \frac{\lambda}{\mu} \right) \quad (49)$$

We consider  $\lambda\mu > 0$ . In this case the above equation is easily solved to give

$$\chi(x) = \sqrt{\frac{\lambda}{\mu}} \tanh(\sqrt{\lambda\mu} x) \quad (50)$$

The pair  $\phi = 0$  and  $\chi$  in (50) is the pair of non-BPS solutions that we have already found. Here, however, we found the non-BPS solution as an explicit solution of the new first-order differential equations in systems of coupled real scalar fields. Although this is a non-BPS solution, we have already shown in Sec. II that its energy is composed of equal portions of gradient (g) and potential (p) contributions. In terms of densities we have, explicitly

$$g_1(x) = p_1(x) = \frac{1}{2}\lambda^2 \text{sech}^4 \left( \sqrt{\lambda\mu} x \right) \quad (51)$$

We can now understand this feature by realizing that although this pair of solutions is non-BPS, in the reduced system where  $\phi \rightarrow 0$ , the  $\chi$  field solution is indeed a BPS solution.

## B. The second model

We consider another model, defined by the superpotential

$$W^{(2)}(\phi, \chi) = \lambda(\phi^2 - 1)\chi \quad (52)$$

This model was also considered in Ref. [28]. The equations of motion are

$$\frac{\partial^2\phi}{\partial t^2} - \frac{\partial^2\phi}{\partial x^2} + 2\lambda^2(\phi^2 - 1)\phi + 4\lambda^2\phi\chi^2 = 0 \quad (53)$$

and

$$\frac{\partial^2\chi}{\partial t^2} - \frac{\partial^2\chi}{\partial x^2} + 4\lambda^2\phi^2\chi = 0 \quad (54)$$

For static fields the energy is minimized for configurations that obey the first-order equations

$$\frac{d\phi}{dx} = 2\lambda\phi\chi \quad (55)$$

$$\frac{d\chi}{dx} = \lambda(\phi^2 - 1) \quad (56)$$

The model presents two vacuum states, given by  $(\pm 1, 0)$ . In contraposition with the former model, however, this new model presents no BPS sector, because the function (52) obeys  $W^{(2)}(\phi^2 = 1, \chi) = 0$ , and then gives  $|\Delta W^{(2)}| = 0$ . This means that the first-order equations (55) and (56) present no topological solutions connecting the two vacuum states. On the other hand, the vacuum states  $(\pm 1, 0)$  can be connected by topological but non-BPS solutions. The explicit form of the solutions is given by

$$\phi(x) = \pm \tanh(\lambda x) \quad (57)$$

$$\chi(x) = 0 \quad (58)$$

The energy or tension of the solution is

$$t_{nBPS}^2 = (4/3)|\lambda| \quad (59)$$

This result reproduces the value presented by the similar one-component BPS solution (40) and (41) of the first model.

We compare this model with the first one to see that it provides a nice way to understand how the BPS and non-BPS solutions behave. We notice that

$$W_{\phi\phi}^{(2)} = 2\lambda\chi, \quad W_{\chi\chi}^{(2)} = 0, \quad W_{\phi\chi}^{(2)} = 2\lambda\phi \quad (60)$$

There is only one way to make  $W^{(2)}$  harmonic, which implies setting  $\chi \rightarrow 0$ . The new first-order equations correspond to the equations (23) and (24) for  $W^{(2)}$ , in the limit  $\chi \rightarrow 0$ . They give

$$\frac{d\phi}{dx} = \lambda(\phi^2 - 1) \quad (61)$$

This is solved by

$$\phi(x) = -\tanh(\lambda x) \quad (62)$$

The pair of solutions formed by  $\chi = 0$  and  $\phi$  as in Eq. (62) is the pair of non-BPS solutions that we have already found for this model. This is another example where one gets non-BPS solutions as solutions to first-order differential equations. This is perhaps the most natural way of understanding why this non-BPS solution has energy evenly distributed into its gradient and potential portions. In terms of energy densities we have

$$g_2(x) = p_2(x) = \frac{1}{2}\lambda^2 \text{sech}^4(\lambda x) \quad (63)$$

### C. The third model

Let us now consider another model, defined by the superpotential

$$W^{(3)}(\phi, \chi) = -\lambda\phi + \frac{1}{3}\mu\phi^3 - \mu\phi\chi^2 \quad (64)$$

This model has the first-order equations

$$\frac{d\phi}{dx} = -\lambda + \mu\phi^2 - \mu\chi^2 \quad (65)$$

$$\frac{d\chi}{dx} = -2\mu\phi\chi \quad (66)$$

The model has only two minima, and for  $\lambda/\mu > 0$  they are  $(\pm\sqrt{\lambda/\mu}, 0)$ . They give

$$W^{(3)}(\pm\sqrt{\lambda/\mu}, 0) = \mp\frac{2}{3}\lambda\sqrt{\frac{\lambda}{\mu}} \quad (67)$$

and define a BPS sector. The explicit BPS solution is given by

$$\phi(x) = -\sqrt{\frac{\lambda}{\mu}} \tanh\left(\sqrt{\lambda\mu}x\right), \quad (68)$$

together with  $\chi = 0$ . We deal with the first-order equations to get

$$\chi\left(\phi^2 - \frac{\lambda}{\mu} - \frac{1}{3}\chi^2\right) = 0 \quad (69)$$

This restriction constrains the orbits in the  $(\phi, \chi)$  plane in such a way that no finite orbit can connect the two minima, unless in the case  $\chi = 0$ , in which one reproduces the topological solution just obtained. This model has a single topological sector, and presents no family of topological solutions, like the family (42) and (43) obtained in the first model.

We use  $W^{(3)}$  to obtain

$$W_{\phi\phi}^{(3)} = 2\mu\phi, \quad W_{\chi\chi}^{(3)} = -2\mu\phi, \quad W_{\phi\chi}^{(3)} = -2\mu\chi \quad (70)$$

We see that  $W^{(3)}$  is harmonic. This means that we have another pair of first-order equations that come from (23) and (24). It is

$$\frac{d\phi}{dx} = 2\mu\phi\chi \quad (71)$$

$$\frac{d\chi}{dx} = -\lambda - \mu\chi^2 + \mu\phi^2 \quad (72)$$

We think of this pair as appearing from another function,  $\widetilde{W}^{(3)}$ , as defined in the Eqs. (26) and (27). We get

$$\widetilde{W}^{(3)} = -\lambda\chi - \frac{1}{3}\mu\chi^3 + \mu\phi^2\chi \quad (73)$$

We notice that  $\widetilde{W}^{(3)}$  vanishes along the line  $\chi = 0$  where the former sector was explicitly constructed.

We can use  $\widetilde{W}^{(3)}$  to write  $\widetilde{W}_{\phi\phi}^{(3)} = 2\mu\chi$ ,  $\widetilde{W}_{\chi\chi}^{(3)} = -2\mu\chi$ , and  $\widetilde{W}_{\phi\chi}^{(3)} = 2\mu\phi$ , showing that  $\widetilde{W}^{(3)}$  is also harmonic, as expected. As we have suggested in Sec. II, we use the complex superpotential  $\mathcal{W}^{(3)} = W^{(3)} + i\widetilde{W}^{(3)}$  and the complex field  $\varphi = \phi + i\chi$ . We change notation and write

$$\mathcal{W}_2(\varphi) = \lambda\varphi - \frac{1}{3}\mu\varphi^3 \quad (74)$$

as the superpotential of the third model. The new notation uses the subscript  $N$  in  $\mathcal{W}_N$  to identify the complex superpotential that presents the  $Z_N$  symmetry – see Sec. VB for further details. We use  $\mathcal{W}_2$  to get, in the vacuum states  $\bar{\varphi}_k$ ,  $k = 1, 2$

$$\mathcal{W}_2(\bar{\varphi}_1) = -\frac{2}{3}\lambda\sqrt{\frac{\lambda}{\mu}} \quad (75)$$

$$\mathcal{W}_2(\bar{\varphi}_2) = \frac{2}{3}\lambda\sqrt{\frac{\lambda}{\mu}} \quad (76)$$

or better

$$\mathcal{W}_2(\bar{\varphi}_k) = -\frac{2}{3}\lambda\sqrt{\frac{\lambda}{\mu}}e^{2\pi i\frac{k-1}{2}} \quad k = 1, 2 \quad (77)$$

We use this result to obtain the tensions

$$t_{jk}^{(2)} = |\mathcal{W}_2(\bar{\varphi}_j) - \mathcal{W}_2(\bar{\varphi}_k)| \quad (78)$$

In the present case there is a single topological sector, with tension

$$t_1^{(2)} = \frac{4}{3}|\lambda|\sqrt{\frac{\lambda}{\mu}} \quad (79)$$

Here we use  $t_n^{(N)}$  to identify tensions in models with complex superpotentials having the  $Z_N$  symmetry – see Sec. VB for more details.

#### D. The fourth model

We consider another model, defined by the superpotential

$$W^{(4)}(\phi, \chi) = \bar{\lambda}\phi + \bar{\mu}\chi - \frac{1}{4}\lambda\phi^4 - \frac{1}{4}\lambda\chi^4 + \frac{3}{2}\lambda\phi^2\chi^2 \quad (80)$$

This model is similar to models already investigated in Ref. [4]. The equations of motion are

$$\frac{d^2\phi}{dx^2} = 6\bar{\mu}\lambda\phi\chi - 3\bar{\lambda}\lambda(\phi^2 - \chi^2) - 6\lambda^2\phi(\chi^2 - 3\phi^2)\chi^2 + 3\lambda^2\phi(\phi^2 - 3\chi^2)(\phi^2 - \chi^2) \quad (81)$$

$$\frac{d^2\chi}{dx^2} = 6\bar{\lambda}\lambda\phi\chi - 3\bar{\mu}\lambda(\chi^2 - \phi^2) - 6\lambda^2\phi^2(\phi^2 - 3\chi^2)\chi + 3\lambda^2(\chi^2 - 3\phi^2)(\chi^2 - \phi^2)\chi \quad (82)$$

These equations are solved by field configurations that obey the first-order equations

$$\frac{d\phi}{dx} = \bar{\lambda} - \lambda\phi(\phi^2 - 3\chi^2) \quad (83)$$

$$\frac{d\chi}{dx} = \bar{\mu} - \lambda\chi(\chi^2 - 3\phi^2) \quad (84)$$

The minima of the potential obey

$$\phi(\phi^2 - 3\chi^2) = \frac{\bar{\lambda}}{\lambda} \quad (85)$$

$$\chi(\chi^2 - 3\phi^2) = \frac{\bar{\mu}}{\lambda} \quad (86)$$

Interesting cases are obtained with  $\bar{\mu} = 0$ , and with  $\bar{\lambda} = 0$ . They give similar models, and we consider the case  $\bar{\mu} = 0$ . We use  $\bar{\phi}^3 = \bar{\lambda}/\lambda$ , and the minima now obey

$$\phi(\phi^2 - 3\chi^2) = \bar{\phi}^3 \quad (87)$$

$$\chi(\chi^2 - 3\phi^2) = 0 \quad (88)$$

The minima are given by  $(\phi_i, \chi_i)$ ,  $i = 1, 2, 3$ , where

$$\phi_1 = \bar{\phi}, \quad \chi_1 = 0 \quad (89)$$

$$\phi_2 = \phi_3 = -\frac{1}{2}\bar{\phi}, \quad \chi_2 = -\chi_3 = \frac{\sqrt{3}}{2}\bar{\phi} \quad (90)$$

They form a triangle in the  $(\phi, \chi)$  plane. The ratio  $\bar{\lambda}/\lambda$  specifies the vacuum states. For instance, for  $\bar{\lambda} = \lambda$  we get the minima at

$$(1, 0), \quad \left(-\frac{1}{2}, \pm\frac{1}{2}\sqrt{3}\right) \quad (91)$$

The minima are equidistant from each other. The triangle they form is equilateral, and the symmetry is the  $Z_3$  symmetry. The distance between the minima is  $d = \sqrt{3}|\bar{\phi}|$ , and depend on the ratio  $\bar{\lambda}/\lambda$ . The function  $W^{(4)}$  is changed to, for  $\bar{\mu} = 0$ ,

$$W^{(5)} = \bar{\lambda}\phi - \frac{1}{4}\lambda\phi^4 - \frac{1}{4}\lambda\chi^4 + \frac{3}{2}\lambda\phi^2\chi^2 \quad (92)$$

The equations of motion are solved by the first-order differential equations

$$\frac{d\phi}{dx} = \lambda[\bar{\phi}^3 - \phi(\phi^2 - 3\chi^2)] \quad (93)$$

$$\frac{d\chi}{dx} = -\lambda\chi(\chi^2 - 3\phi^2) \quad (94)$$

We use Eq. (92) to get

$$W^{(5)}(\phi_1, \chi_1) = \frac{3}{4}\lambda\bar{\phi}^4 \quad (95)$$

$$W^{(5)}(\phi_2, \chi_2) = W^{(5)}(\phi_3, \chi_3) = -\frac{3}{8}\lambda\bar{\phi}^4 \quad (96)$$

We notice that  $W^{(4)}$  (and also  $W^{(5)}$ ) is harmonic. This means that the potential of this model can be obtained by another superpotential, given by

$$\widetilde{W}^{(4)}(\phi, \chi) = -\bar{\mu}\phi + \bar{\lambda}\chi - \lambda\phi^3\chi + \lambda\phi\chi^3 \quad (97)$$

We set  $\bar{\mu} = 0$  to get

$$\widetilde{W}^{(5)}(\phi, \chi) = \bar{\lambda}\chi - \lambda\phi^3\chi + \lambda\phi\chi^3 \quad (98)$$

The corresponding first-order equations are

$$\frac{d\phi}{dx} = \lambda\chi(\chi^2 - 3\phi^2) \quad (99)$$

$$\frac{d\chi}{dx} = \lambda[\bar{\phi}^3 - \phi(\phi^2 - 3\chi^2)] \quad (100)$$

Evidently, the minima are  $(\phi_i, \chi_i)$ ,  $i = 1, 2, 3$ , the same minima already obtained in Eqs. (89) and (90). However,  $\widetilde{W}^{(5)}$  behaves differently

$$\widetilde{W}^{(5)}(\phi_1, \chi_1) = 0 \quad (101)$$

$$\widetilde{W}^{(5)}(\phi_2, \chi_2) = -\widetilde{W}^{(5)}(\phi_3, \chi_3) = \frac{3}{8}\sqrt{3}\lambda\bar{\phi}^4 \quad (102)$$

This model leads to the model recently considered in Refs. [21,22]. We proceed like in the form model to get the complex superpotential

$$\mathcal{W}_3(\varphi) = \bar{\lambda} \varphi - \frac{1}{4} \lambda \varphi^4 \quad (103)$$

The field  $\varphi$  is complex,  $\varphi = \phi + i\chi$ . In Ref. [21] one considers the case  $\bar{\lambda} = \lambda = 1$ . In this case the potential is a particular case of the potential introduced above. The superpotential can be seen as  $\mathcal{W}_3 = W^{(5)} + i\widetilde{W}^{(5)}$ , and this allows obtaining

$$\mathcal{W}_3(\bar{\varphi}_1) = \frac{3}{4} \lambda \bar{\phi}^4 \quad (104)$$

$$\mathcal{W}_3(\bar{\varphi}_2) = \frac{3}{4} \lambda \bar{\phi}^4 \left( -\frac{1}{2} + i\frac{1}{2}\sqrt{3} \right) \quad (105)$$

$$\mathcal{W}_3(\bar{\varphi}_3) = \frac{3}{4} \lambda \bar{\phi}^4 \left( -\frac{1}{2} - i\frac{1}{2}\sqrt{3} \right) \quad (106)$$

or better

$$\mathcal{W}_3(\bar{\varphi}_k) = \frac{3}{4} \lambda \bar{\phi}^4 e^{2\pi i \frac{k-1}{3}}, \quad k = 1, 2, 3 \quad (107)$$

We use this result to write

$$t_{jk}^{(3)} = |\mathcal{W}_3(\bar{\varphi}_j) - \mathcal{W}_3(\bar{\varphi}_k)| \quad (108)$$

The three tensions degenerate to the single value

$$t_1^{(3)} = \frac{3}{4} \sqrt{3} |\lambda| \bar{\phi}^4 \quad (109)$$

#### IV. STABILITY

In this Sec. IV we deal with issues concerning stability of the topological solutions in (1, 1) dimensions. We follow Ref. [15], recalling that the linear stability also shows how the bosonic fields behave in the background of the classical solutions. We examine linear stability for two coupled real scalar fields using  $\phi(x, t) = \bar{\phi}(x) + \eta(x, t)$  and  $\chi(x, t) = \bar{\chi}(x) + \xi(x, t)$ . Here

$$\eta(x, t) = \sum_n \eta_n(x) \cos(w_n t) \quad (110)$$

$$\xi(x, t) = \sum_n \xi_n(x) \cos(w_n t) \quad (111)$$

are the fluctuations around the static solutions  $\bar{\phi}$  and  $\bar{\chi}$ . We use the equations of motion to get the equation for stability

$$\left( -\hat{1} \frac{d^2}{dx^2} + U \right) \begin{pmatrix} \eta_n \\ \xi_n \end{pmatrix} = w_n^2 \begin{pmatrix} \eta_n \\ \xi_n \end{pmatrix} \quad (112)$$

For  $w_n^2 \geq 0$  ( $w_n^2 < 0$ ) we have stable (unstable) solutions. Here  $\hat{1}$  is the  $2 \times 2$  identity matrix and

$$U = \begin{pmatrix} \bar{V}_{\phi\phi} & \bar{V}_{\phi\chi} \\ \bar{V}_{\chi\phi} & \bar{V}_{\chi\chi} \end{pmatrix} \quad (113)$$

The bar over the potential means that after obtaining the derivatives, we should substitute the fields  $\phi$  and  $\chi$  by their classical static values  $\bar{\phi}(x)$  and  $\bar{\chi}(x)$ .

We consider the first model first. In this case the explicit calculation gives to the matrix  $U^{(1)}$  the elements  $U_{ij}^{(1)} = 2\mu^2 m_{ij}$ , where

$$m_{11} = -\left(\frac{\lambda}{\mu}\right)^2 + 3\left(\frac{\lambda}{\mu}\right)^2 \bar{\phi}^2 + \left(\frac{\lambda}{\mu} + 2\right) \bar{\chi}^2 \quad (114)$$

$$m_{12} = m_{21} = 2\left(\frac{\lambda}{\mu} + 2\right) \bar{\phi} \bar{\chi} \quad (115)$$

$$m_{22} = -\frac{\lambda}{\mu} + \left(\frac{\lambda}{\mu} + 2\right) \bar{\phi}^2 + 3\bar{\chi}^2 \quad (116)$$

We use the first-order equations (35) and (36) to introduce the first-order operators

$$S = \hat{1} \frac{d}{dx} + 2\mu \begin{pmatrix} \frac{\lambda}{\mu} \bar{\phi} & \bar{\chi} \\ \bar{\chi} & \bar{\phi} \end{pmatrix} \quad (117)$$

and

$$S^\dagger = -\hat{1} \frac{d}{dx} + 2\mu \begin{pmatrix} \frac{\lambda}{\mu} \bar{\phi} & \bar{\chi} \\ \bar{\chi} & \bar{\phi} \end{pmatrix} \quad (118)$$

These operators allow writing  $H_1 = S^\dagger S$ , where  $H_1$  is the Hamiltonian corresponding to the first model

$$H_1 = -\hat{1} \frac{d^2}{dx^2} + U^{(1)} \quad (119)$$

This factorization  $H_1 = S^\dagger S$  shows that  $H_1$  is positive semi-definite, and so can have no negative eigenvalue. We then conclude that the BPS solutions are stable, since they solve the first-order equations we need to get the first-order operators (117) and (118).

In this first model, the one-component solutions can be solved explicitly. For the BPS pair (40) and (41) we get the following set of discrete eigenvalues: in the first direction, the  $\phi$  direction

$$w_0^{(1,1)} = 0 \quad w_1^{(1,1)} = \sqrt{3\lambda^2} \quad (120)$$

and in the second direction, the  $\chi$  direction

$$w_0^{(1,2)} = 0 \quad (121)$$

For the pair of non-BPS solutions given by  $\phi = 0$  and  $\chi$  in Eq. (45) we get

$$\bar{w}_n^{(1,1)} = \sqrt{\lambda\mu} \left\{ 4 - \left[ \left( n + \frac{1}{2} \right) - \sqrt{2 \left( 2 + \frac{\lambda}{\mu} \right) + \frac{1}{4}} \right]^2 \right\}^{1/2} \quad (122)$$

and

$$\bar{w}_0^{(1,2)} = 0 \quad \bar{w}_1^{(1,2)} = \sqrt{3\lambda\mu} \quad (123)$$

Since  $\lambda/\mu > 0$ , we find the restriction  $0 < \lambda/\mu \leq 1$  on the ratio  $\lambda/\mu$  in order to make the non-BPS solution stable.

We notice that for  $\mu = \lambda$  the eigenvalues  $\bar{w}_n^{(1,1)}$  change to 0 and  $\sqrt{3\lambda^2}$ , and degenerate to the values  $\bar{w}_n^{(1,2)}$ ,  $n = 0, 1$ , given above. This means that the scalar matter splits into two equal portions that present equal BPS states.

Let us now consider the second model. For the pair of non-BPS solutions given by Eqs. (57) and (58) we get the following set of eigenvalues for the bound states, in the first direction

$$w_0^{(2,1)} = 0, \quad w_1^{(2,1)} = \sqrt{3\lambda^2} \quad (124)$$

In the second direction we have

$$w_0^{(2,2)} = \sqrt{[(\sqrt{17} - 1)/2]\lambda^2} \quad (125)$$

$$w_1^{(2,2)} = \sqrt{[(3\sqrt{17} - 5)/2]\lambda^2} \quad (126)$$

Let us now consider the third model. We use the pair obtained with (68) and  $\chi = 0$  to obtain for the bound states the set of eigenvalues, in the first direction

$$w_0^{(3,1)} = 0, \quad w_1^{(3,1)} = \sqrt{3\lambda\mu} \quad (127)$$

and, in the second direction

$$w_0^{(3,2)} = \sqrt{2\lambda\mu} \quad (128)$$

We cannot present explicit investigations concerning stability of solutions of the fourth model, because we do not know any explicit solution in this case. However, we consider stability of the solutions of another model, introduced in Ref. [24]. This model is defined by the superpotential

$$\begin{aligned} W(\phi, \chi) = & \lambda\sqrt{\frac{4}{27}} \left( \chi + \sqrt{\frac{1}{3}} \right)^3 - \lambda \left( \chi + \sqrt{\frac{1}{3}} \right)^2 \\ & + \lambda\phi \left( \chi + \sqrt{\frac{1}{3}} \right)^2 - 3\lambda\phi + \lambda\phi^3 \end{aligned} \quad (129)$$

The system presents the three minima  $(0, \pm\sqrt{4/3})$  and  $(\pm 1, -\sqrt{1/3})$ . They give three BPS sectors, having energies  $|\lambda|$ ,  $3|\lambda|$ , and  $4|\lambda|$ . The highest energy is associated to the sector connecting the minima  $(\pm 1, -\sqrt{1/3})$ . This is the only sector where we can find explicit solutions. They are given by

$$\phi(x) = -\tanh(3\lambda x) \quad (130)$$

$$\chi(x) = -\sqrt{1/3} \quad (131)$$

This pair of solutions represents a straight line orbit in the  $(\phi, \chi)$  plane, connecting the two vacua  $(\pm 1, -\sqrt{1/3})$ . We consider stability of the above solutions. Here the fluctuations decouple and we obtain

$$U_{11} = 9\lambda^2[4 - 6\operatorname{sech}^2(3\lambda x)] \quad (132)$$

$$U_{22} = 9\lambda^2 \left( \frac{8}{9} \right) \left[ 1 + \tanh(3\lambda x) - \frac{5}{4}\operatorname{sech}^2(3\lambda x) \right] \quad (133)$$

The first potential  $U_{11}$  is the modified Pösch-Teller potential. It presents two bound states, with energies

$$w_0 = 0, \quad w_1 = 3\sqrt{3\lambda^2} \quad (134)$$

The second potential  $U_{22}$  is not reflectionless. It supports no bound state, and the continuum starts at zero energy.

## V. FURTHER CONSIDERATIONS

The models investigated above present similar BPS and non-BPS solutions. They provide concrete ways of investigating how the scalar fields behave in the background of BPS and non-BPS solutions. We explore some possibilities in the next Sec. V A. In Sec. V B we investigate intersection of defects.

### A. Entrapment of the other field

In the first model, we can further understand the importance of the topological solutions by investigating the potential  $V_1(\phi, \chi)$ . It is given by

$$\begin{aligned} V_1(\phi, \chi) = & \frac{1}{2}\lambda^2(\phi^2 - 1)^2 + \lambda\mu(\phi^2 - 1)\chi^2 \\ & + \frac{1}{2}\mu^2\chi^4 + 2\mu^2\phi^2\chi^2 \end{aligned} \quad (135)$$

This model presents the one-component BPS solution (40) and (41). We have  $\phi^2 = 1$  outside the BPS defect, and  $\phi = 0$  at  $x = 0$ , at the center of the defect. We then use  $V_1(\phi, \chi)$  to get

$$V_1(\phi \rightarrow 0, \chi) = \frac{1}{2}\mu^2 \left( \chi^2 - \frac{\lambda}{\mu} \right)^2 \quad (136)$$

$$V_1(\phi^2 \rightarrow 1, \chi) = 2\mu^2\chi^2 + \frac{1}{2}\mu^2\chi^4 \quad (137)$$

For  $\lambda/\mu > 0$  the potential (136) shows the presence of spontaneous symmetry breaking in the independent  $\chi$  direction in the  $(\phi, \chi)$  plane. In this case the  $\chi$  field presents squared masses given by

$$m_\chi^2(in) = 4\lambda\mu \quad (138)$$

$$m_\chi^2(out) = 4\mu^2 \quad (139)$$

where *in* and *out* identify the region inside and outside the defect. We see that the ratio of masses is

$$\frac{m_\chi^2(in)}{m_\chi^2(out)} = \frac{\lambda}{\mu} \quad (140)$$

This ratio identifies the region  $0 < \lambda/\mu < 1$  in the space of parameters where the field  $\phi$  entraps the other field. For a given  $\lambda$ , we see that the parameter  $\mu$  controls the ratio of squared masses. Thus, the efficiency of the entrapment depends on  $\mu$ .

This model can be used as a bag model [29], similar to the models in Refs. [30,31]. Here we can further enlarge the model by changing dimensions from (1,1) to (3,1) and making the  $\chi$  field complex, going from the  $Z_2 \times Z_2$  symmetry to the  $Z_2 \times U(1)$ . However, since inside the defect formed by  $\phi(x)$ , the  $\chi$  field still engenders spontaneous symmetry breaking for  $\lambda\mu > 0$ , we can only circumvent the presence of Goldstone bosons when one gauge the related  $U(1)$  symmetry, making it local. The model that emerges presents the symmetry  $Z_2 \times U_1(1)$ . Since we started in (3,1) dimensions, inside the wall the theory is effectively (2,1) dimensional. This is an alternate mechanism for dimensional reduction, and inside the wall the effective theory may very naturally develop the Callan-Harvey effect [40], if one appropriately couples fermions to the second field,  $\chi$ . This scenario seems to appear interesting, and we shall further explore this possibility in a separate report.

The first model is simpler for  $\lambda\mu < 0$ . In this case, spontaneous symmetry breaking no longer appear inside the wall formed by the  $\phi$  field. However, the wall is still of the BPS type. The potential  $V_1(\phi, \chi)$  changes in a way such that the ratio (140) becomes

$$\frac{m_\chi^2(in)}{m_\chi^2(out)} = -\frac{\lambda}{2\mu} \quad (141)$$

This result shows that the topological defect generated by  $\phi$  can still entrap  $\chi$  mesons for  $0 > \lambda/\mu > -2$ , acting like a bag for the elementary excitations of the field  $\chi$ . If we change the symmetry  $Z_2 \times Z_2$  to  $Z_2 \times U(1)$  by making the  $\chi$  field complex, in this case we do not need to make the  $U(1)$  symmetry local, and we can still explore the presence of a global symmetry within the wall. Work in this direction was already presented in Ref. [41], in a model inspired in the work of Ref. [6], with a potential that differs from the one here proposed. We believe that our model may give further insight into the issues that arise in this scenario. Further applications can be done, as for instance in Ref. [42], where one explores the presence of diffuse domain walls at intersecting flat directions within the cosmological scenario. Also, we can follow Ref. [43] to investigate issues concerning hybrid inflation, involving features that requires at least two real scalar fields, the inflaton field and another one, which is in general used to break the symmetry.

The second model is defined with the superpotential (52). It gives the potential

$$V_2(\phi, \chi) = \frac{1}{2}\lambda^2(\phi^2 - 1)^2 + 2\lambda^2\phi^2\chi^2 \quad (142)$$

Here we have

$$V_2(\phi = 0, \chi) = \frac{1}{2}\lambda^2 \quad (143)$$

$$V_2(\phi^2 = 1, \chi) = 2\lambda^2\chi^2 \quad (144)$$

Thus the squared masses associated to the  $\chi$  field are

$$m_\chi^2(in) = 0 \quad (145)$$

$$m_\chi^2(out) = 4\lambda^2 \quad (146)$$

In this case the non-BPS defect always entraps the field  $\chi$ , acting like a bag for the elementary  $\chi$  excitations. Here, however, the  $\chi$  meson is massless inside the bag. This shows that the entrapment is more efficient in this model, although the basic solution, the bag, is of the non-BPS type.

We can investigate the third model similarly. It is defined by the superpotential (64) and we have

$$V_3(\phi, \chi) = \frac{1}{2}\mu^2 \left( \phi^2 - \frac{\lambda}{\mu} \right)^2 - \mu^2 \left( \phi^2 - \frac{\lambda}{\mu} \right) \chi^2 + \frac{1}{2}\mu^2\chi^4 + 2\mu^2\phi^2\chi^2 \quad (147)$$

We can write, for  $\lambda/\mu > 0$ ,

$$V_3(0, \chi) = \frac{1}{2}\mu^2 \left( \chi^2 + \frac{\lambda}{\mu} \right)^2 \quad (148)$$

$$V_3(\pm\sqrt{\lambda/\mu}, \chi) = 2\lambda\mu\chi^2 + \frac{1}{2}\mu^2\chi^4 \quad (149)$$

No spontaneous symmetry breaking appears inside the  $\phi$ -defect anymore, and so the model cannot support defect inside defect. However, the squared masses of the elementary  $\chi$  mesons are

$$\tilde{m}_\chi^2(in) = 2\lambda\mu \quad (150)$$

$$\tilde{m}_\chi^2(out) = 4\lambda\mu \quad (151)$$

We get the ratio

$$\frac{\tilde{m}_{\chi(in)}^2}{\tilde{m}_{\chi(out)}^2} = \frac{1}{2} \quad (152)$$

This ratio does not depend on the parameters  $\lambda$  and  $\mu$ , but the topological defect may also entrap  $\chi$  mesons. This is another model, in which the topological state may simulate a bag to entrap the elementary excitations of the other field. In this case, however, the efficiency of the entrapment can no longer be controlled by the parameters that defines the model.

The second and third models may also be immersed in the (3,1) dimensional space-time. This immersion provide alternative ways to investigate the behavior of the current generated by making the second field complex, as commented above. They give similar scenarios

for charged walls, and may present distinct physical contents.

Other applications include the diverse issues recently investigated in Refs. [12–15,27,44]. We can, for instance, enlarge the models in order to break the symmetry and/or the supersymmetry. This possibility may give rise to Fermi balls [27], Fermi disks [14], and other charged objects [44], which depend on the particular space-time dimension one starts with, and on the parameters that define the terms added to allow the symmetry breaking. We can also follow Refs. [12,13,15] to extend the scenario of nested defects to the case of nested network of defects. This picture follows as a direct generalization of the result of Ref. [15], which shows explicitly that defects may nest defects if the model engenders the  $Z_2 \times Z_2$  symmetry in systems of two real scalar fields. As we are going to see below, to have intersection of defects we must necessarily enlarge the  $Z_2$  symmetry to at least the  $Z_3$  one. For this reason, we can think of a model that presents the  $Z_2 \times Z_3$  symmetry, composed of three real scalar fields, one presenting the  $Z_2$  symmetry, and the other two controlling the  $Z_3$  symmetry. In (3, 1) space-time dimensions the first field engenders the  $Z_2$  symmetry, and we can certainly get to the case where it may give rise to a domain wall, which may nest the two other fields in its interior. Within this scenario, if the  $Z_3$  symmetry related to the second and third fields is still effective we may nest a planar network of defects inside domain walls. We take advantage of the model investigated in Ref. [24] to present a model that seems to work correctly. This model is defined by

$$V(\psi, \phi, \chi) = \frac{2}{3}\lambda^2 \left( \psi^2 - \frac{9}{4} \right)^2 - \lambda^2 \psi^2 (\phi^2 + \chi^2) + \lambda^2 (\phi^2 + \chi^2)^2 - \lambda^2 \phi (\phi^2 - 3\chi^2) \quad (153)$$

It behaves standardly in (3, 1) space-time dimensions and is such that  $V(\psi) = V(\psi, 0, 0)$  obeys

$$V(\psi) = \frac{2}{3}\lambda^2 \left( \psi^2 - \frac{9}{4} \right)^2 \quad (154)$$

We consider that the field  $\psi = \psi(x)$  depends only on  $x$ . Thus, it supports BPS defects with the explicit form

$$\psi(x) = -\frac{3}{2} \tanh \left( \sqrt{3} \lambda x \right) \quad (155)$$

The corresponding energy density is  $3\sqrt{3}\lambda^2$ . We also notice that the potentials  $V_{in}(\phi, \chi) = V(0, \phi, \chi)$  and  $V_{out}(\phi, \chi) = V(\pm 3/2, \phi, \chi)$  are such that

$$V_{in}(\phi, \chi) = \frac{27}{8}\lambda^2 + \lambda^2(\phi^2 + \chi^2)^2 - \lambda^2\phi(\phi^2 - 3\chi^2) \quad (156)$$

and

$$V_{out}(\phi, \chi) = \lambda^2(\phi^2 + \chi^2)^2 - \lambda^2\phi(\phi^2 - 3\chi^2) - \frac{9}{4}\lambda^2(\phi^2 + \chi^2) \quad (157)$$

We see that the  $Z_3$  symmetry of the pair of fields  $(\phi, \chi)$  is preserved both inside and outside the domain wall generated by the first field,  $\psi$ . In the region inside the domain wall,  $V_{in}(\phi, \chi)$  has minima at the points

$$\left( \frac{3}{4}, 0 \right), \quad \left( -\frac{3}{8}, \pm \frac{3}{8}\sqrt{3} \right) \quad (158)$$

In this region inside the domain wall the squared masses corresponding to the two mesons are

$$m_\phi^2(in) = \frac{9}{4}\lambda^2 \quad (159)$$

$$m_\chi^2(in) = \frac{27}{4}\lambda^2 \quad (160)$$

In the region outside the domain wall,  $V_{out}(\phi, \chi)$  has the minima [24]

$$\left( \frac{3}{2}, 0 \right), \quad \left( -\frac{3}{4}, \pm \frac{3}{4}\sqrt{3} \right) \quad (161)$$

In this case the squared masses are  $m_\phi^2(out) = m_\chi^2(out) = (27/2)\lambda^2$ . These results show that the field  $\psi$  engenders an efficient mechanism for the entrapment of the pair of fields  $(\phi, \chi)$  in this model. We shall further explore this and other related issues in another work.

## B. Intersection of defects

The process of intersection of defects was already explored in Ref. [20], in the case of supersymmetric field theories. There, the basic idea was to show that the intersection of two extended objects is energetically admissible when it can be seen as a reaction that occurs exothermically. This may be translated into the expression  $t_{ik} < t_{ij} + t_{jk}$ , where  $t_{ik}$ ,  $t_{ij}$ , and  $t_{jk}$  are the energies or tensions associated to the fusion of the two defects, and to the individuals defects, respectively. The crucial point here is that in supersymmetric theories the topological charge  $\mathcal{T}$  of the defect appears as a central charge, and for BPS states one gets  $t = |\mathcal{T}|$ . If one uses  $t_{ij} = |\mathcal{T}_{ij}|$ ,  $t_{jk} = |\mathcal{T}_{jk}|$ , and  $t_{ik} = |\mathcal{T}_{ij} + \mathcal{T}_{jk}|$  the triangle inequality  $t_{ik} \leq t_{ij} + t_{jk}$  follows naturally. This triangle inequality is strictly valid in supersymmetric systems described by complex superpotentials, whose values at the vacuum states define points in the complex plane, not aligned into a straight-line segment.

The fourth model is the supersymmetric model that opens the possibility for the presence of stable intersection of extended objects, giving rise to a triple junction of BPS states, as recently shown in Ref. [21] – see also Refs. [22,23]. This model was considered in Sec III D, and

the basic model is given by  $\varphi - (1/4)\varphi^4$ . Here, however, we consider the case

$$\mathcal{W}_N = \bar{\lambda}\varphi - \frac{1}{N+1}\lambda\varphi^{(N+1)} \quad (162)$$

with  $\lambda$  and  $\bar{\lambda}$  real parameters. This model presents the  $Z_N$  symmetry. The vacuum states are singular points of the superpotential. They obey  $\varphi^N = \bar{\lambda}/\lambda$ , and the  $N$  solutions are, using  $\bar{\lambda} = a^N\lambda$  with  $a$  real and positive,

$$\bar{\varphi}_k = a e^{2\pi i[(k-1)/N]}, \quad k = 1, 2, \dots, N. \quad (163)$$

The topological sectors connect pairs of adjacent vacua, and in general the number of BPS sectors is  $N(N-1)/2$ . Their energies or tensions are given in terms of the values of the superpotential in the singular points, that is

$$t_{ij}^{(N)} = |\mathcal{W}_N(\bar{\varphi}_i) - \mathcal{W}_N(\bar{\varphi}_j)| \quad (164)$$

The tensions can be classified according to the integer  $n$ ,  $n = 1, 2, \dots, \leq [N/2]$ , where  $[N/2]$  stands for the greatest integer not greater than  $N/2$  itself. These tensions have the explicit values

$$t_n^{(N)} = \frac{Na^{(N+1)}}{N+1} |\lambda| \sqrt{2 \left[ 1 - \cos \left( 2\pi \frac{n}{N} \right) \right]} \quad (165)$$

The integer  $n$  identifies topological sectors described via the connection between a given vacuum, and its  $n - th$  neighbor:  $n = 1$  for connections between first neighbors,  $n = 2$  for second neighbors, and so forth. We can check that these tensions are ordered in the form  $t_k^{(N)} < t_{k+1}^{(N)}$ , for  $k = 1, \dots, < [N/2]$ , and  $N \geq 4$ . This order also shows that the direct connection between two vacuum states is always less energetic than any other possible connection. For instance,  $t_2^{(N)} < 2t_1^{(N)}$ ,  $N \geq 4$ , and  $t_3^{(N)} < t_2^{(N)} + t_1^{(N)}$ ,  $N \geq 6$ , and so forth.

More recently, in Ref. [24] we considered another model. The model is defined by the potential

$$V(\phi, \chi) = \lambda^2 \phi^2 \left( \phi^2 - \frac{9}{4} \right) + \lambda^2 \chi^2 \left( \chi^2 - \frac{9}{4} \right) + 2\lambda^2 \phi^2 \chi^2 - \lambda^2 \phi (\phi^2 - 3\chi^2) + \frac{27}{8} \lambda^2 \quad (166)$$

It presents the  $Z_3$  symmetry, but it is described by a potential that cannot be written in terms of some superpotential. In this case the key issue relies on finding a way out of supersymmetry to show that the fusion of defects still occurs exothermically. In the supersymmetric case one can use interesting properties to make the reasoning naturally simple. In the non-supersymmetric case, however, we have found non-BPS solutions that presents the interesting property of having gradient and potential portions of the energy evenly distributed to compose the total energy of the defect. As we have shown, such a property is also shared by all the BPS solutions, and so we can use it to present a new reasoning, that works

within and beyond the context of supersymmetry. The reasoning follows from the topological current presented in Eq. (30). Here we have

$$\rho(x) = \begin{pmatrix} \phi'(x) \\ \chi'(x) \end{pmatrix} \quad (167)$$

Thus  $\rho^t \rho = 2g(x)$ , and for static solutions that presents equal gradient and potential portions we get  $\rho^t \rho = g(x) + p(x) = \varepsilon(x)$ , or better

$$t_{ij} = \int_{-\infty}^{\infty} dx \rho_{ij}^t \rho_{ij} \quad (168)$$

We consider fusion of two defects in the model investigated in Ref. [24]. The topological defects there obtained obey  $g(x) = p(x)$ . Thus, we can use

$$(\rho_{ij} + \rho_{jk})^t (\rho_{ij} + \rho_{jk}) = \rho_{ij}^t \rho_{ij} + \rho_{jk}^t \rho_{jk} + \rho_{ij}^t \rho_{jk} + \rho_{jk}^t \rho_{ij} \quad (169)$$

Also, we take advantage of the symmetry of the model to see that if the pair  $(\phi, \chi)$  represents a solution in a given sector, all the other solutions can be obtained by rotating the solution according to the  $Z_3$  symmetry. This means that we can write

$$\begin{pmatrix} \phi'_{ij}(x) \\ \chi'_{ij}(x) \end{pmatrix} = \begin{pmatrix} \cos(\alpha_{ij}) & \sin(\alpha_{ij}) \\ -\sin(\alpha_{ij}) & \cos(\alpha_{ij}) \end{pmatrix} \begin{pmatrix} \phi'(x) \\ \chi'(x) \end{pmatrix} \quad (170)$$

Here  $\alpha_{ij}$  is the angle between the given solution  $(\phi, \chi)$  and the solution  $(\phi_{ij}, \chi_{ij})$ . In the  $Z_3$  model under consideration  $\alpha_{ij}$  can only be  $2\pi/3$  and  $4\pi/3$ . We now use (168), (169), and (170) to obtain  $t_{ik} < t_{ij} + t_{jk}$ . This result shows that the three-junction in the model under consideration occurs exothermically.

## VI. NETWORKS OF DEFECTS

The recent Refs. [21–23] have introduced investigations concerning defect junctions and networks in supersymmetric systems, and now we turn our attention to this possibility. We consider junctions in the plane, which may give rise to planar networks of defects. To implement this possibility we work in the  $(2, 1)$  space-time, in the plane  $(x, y)$ . We identify the axes  $(x, y)$  with the axes  $(\phi, \chi)$  of the space of configurations. We illustrate this situation by considering the model defined by the potential in Eq. (166). The topological solutions in the planar case are [24]

$$\phi_{(2,3)}^{\pm} = -\frac{3}{4} \quad (171)$$

$$\chi_{(2,3)}^{\pm} = \pm \frac{3}{4} \sqrt{3} \tanh \left( \sqrt{\frac{27}{8}} \lambda y \right) \quad (172)$$

and

$$\phi_{(1,2)}^{\pm} = \frac{3}{8} \left[ 1 \mp 3 \tanh \left( \frac{1}{2} \sqrt{\frac{27}{8}} \lambda (y + \sqrt{3}x) \right) \right] \quad (173)$$

$$\chi_{(1,2)}^{\pm} = \frac{3}{8} \sqrt{3} \left[ 1 \pm \tanh \left( \frac{1}{2} \sqrt{\frac{27}{8}} \lambda (y + \sqrt{3}x) \right) \right] \quad (174)$$

and

$$\phi_{(1,3)}^{\pm} = \frac{3}{8} \left[ 1 \pm 3 \tanh \left( \frac{1}{2} \sqrt{\frac{27}{8}} \lambda (y - \sqrt{3}x) \right) \right] \quad (175)$$

$$\chi_{(1,3)}^{\pm} = -\frac{3}{8} \sqrt{3} \left[ 1 \mp \tanh \left( \frac{1}{2} \sqrt{\frac{27}{8}} \lambda (y - \sqrt{3}x) \right) \right] \quad (176)$$

They may be used to represent the three-junction in the thin wall approximation.

Let us consider the first model, in the case  $\lambda/\mu > 0$ . The minima are at  $v_1 = (1, 0)$ ,  $v_2 = (0, \sqrt{\lambda/\mu})$ ,  $v_3 = (-1, 0)$ , and  $v_4 = (0, -\sqrt{\lambda/\mu})$ . The energies or tensions of the BPS and non-BPS sectors are  $t_{BPS}^1 = 2\bar{t}_{BPS}^1 = \sqrt{(\mu/\lambda)}t_{nBPS}^1 = (4/3)|\lambda|$ . For a given  $\lambda$ , the value of  $\mu$  allows obtaining three distinct situations. The first concerns the case  $\mu > \lambda$ . In this case the minima give rise to an array of defects of the form shown in FIG. 1, in the thin wall approximation.

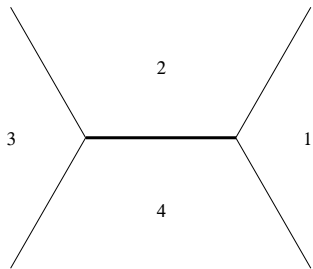


FIG. 1. A possible array of defects, as suggested by the first model of Sec. III A in the case of  $\lambda/\mu < 1$ . The vacuum states are represented by  $v_1 = 1, v_2 = 2, v_3 = 3$ , and  $v_4 = 4$ , and the thinner and thicker lines stand for BPS and non-BPS defects, respectively.

The second case concerns  $\mu = \lambda$ , and the third one  $\mu < \lambda$ . In the thin wall approximation they are shown in FIG. 2, and in FIG. 3, respectively. The second case seems to give an intersection of four half-defects, but this is not true since for  $\mu = \lambda$  the two fields decouple. Thus, the apparent intersection of four half-defects represents in fact the uninteresting case of two non-intersecting defects.

The first and third cases seem to be dual to each other, since they are linked by the interchange  $\lambda \leftrightarrow \mu$ . This duality is very much like the  $s \leftrightarrow t$  duality that the diagrams depicted in FIG. 1 and in FIG. 3 remember. This scenario excludes the self-dual case, where  $\mu = \lambda$ .

The basic diagrams of FIG. 1 and FIG. 3 can be used to generate planar networks of defects. We can generate a

network in the two following ways. The s-network, which appears for  $\lambda/\mu < 1$ , and the t-network, for  $\lambda/\mu > 1$ . They are depicted in FIG. 4 and in FIG. 5, in the case of regular hexagonal networks in the thin wall approximation. In the first case we impose that the triangle with vertices  $v_1, v_2, v_4$  is equilateral. This gives  $\lambda/\mu = 1/3$ . In the second case we impose that the triangle with vertices  $v_1, v_2, v_3$  is equilateral. It gives  $\lambda/\mu = 3$ , the result we should expect from duality. We notice that the first (second) imposition subdivides the distance between the horizontal (vertical) vacua into three equal pieces, which is the condition for the formation of a network of regular hexagons.

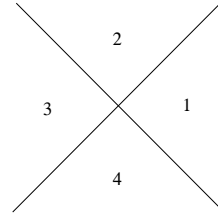


FIG. 2. Another array of defects, suggested by the first model of Sec. III A in the case of  $\lambda/\mu = 1$ .

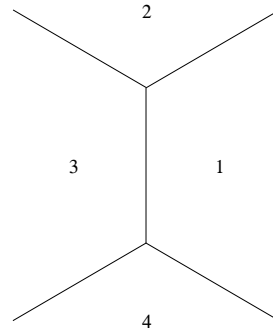


FIG. 3. Another possible array of defects, as suggested by the first model of Sec. III A in the case of  $\lambda/\mu > 1$ .

For  $\mu = 3\lambda$ , we have two sides of the hexagon formed by non-BPS states, with tension  $\sqrt{(1/3)}t_{BPS}^1$ . The other four sides are formed by BPS states, with tension  $(1/2)t_{BPS}^1$ . For  $\mu = (1/3)\lambda$ , two sides of the hexagon are formed by BPS states, with tension  $t_{BPS}^1$ , and the other four sides are also formed by BPS states, with tension  $(1/2)t_{BPS}^1$ .

We think of a planar network of defects. We notice that a t-network means  $\lambda/\mu > 1$ , and this allows hexagonal networks with two distinct BPS states, having two different tensions,  $t_{BPS}^1$  and  $\bar{t}_{BPS}^1 = (1/2)t_{BPS}^1$ , showing that each three-junction of this t-network is at the threshold of stability. For  $\lambda/\mu < 1$ , in the case of s-networks, however, the situation is different since now

we must have two non-BPS states to build the hexagonal cell. Since the ratio  $\lambda/\mu < 1$  controls the energy of the non-BPS state, every three-junction may obey the inequality  $t_{ij} < t_{jk} + t_{ki}$ .

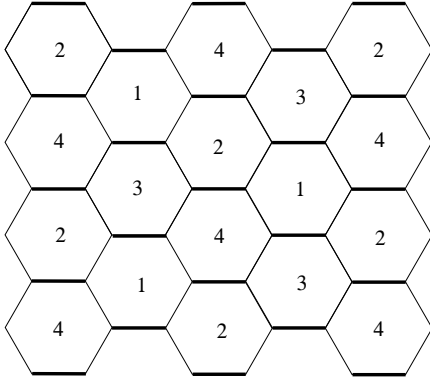


FIG. 4. The s-network, depicted as a regular hexagonal network of defects in the case of  $\lambda/\mu = 1/3$ . The thicker lines represent non-BPS states.

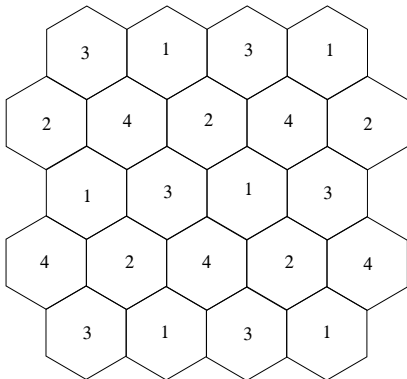


FIG. 5. The t-network, depicted as a regular hexagonal network of defects in the case of  $\lambda/\mu = 3$ .

We can consider the case where  $t_{nBPS}^1 = \bar{t}_{BPS}^1$ . This gives  $\mu = 4\lambda$  and the tensions degenerate to the single value  $(2/3)|\lambda|$ . The hexagonal cell is no longer regular. The angle between the two BPS states changes from  $\alpha = 120$  to  $\alpha = 2\theta$ , where  $\theta$  is slightly lesser than 63.5 degrees. We notice that we cannot make the tensions and angles degenerate simultaneously, and this indicates instability of the suggested networks.

Effects that contribute to stabilize the network may appear when we go beyond the classical level and introduce the quantum corrections, since the quantum contributions may modify the classical scenario. For instance, in the case  $\lambda/\mu > 1$ , in a t-network all the defects are BPS defects, and their energies or tensions are protected against receiving quantum corrections. On the

other hand, for  $\lambda/\mu < 1$ , in the case of a s-network there are non-BPS states whose tensions are not protected and may receive quantum corrections, changing the classical value  $t_{nBPS}^1$ , contributing to stabilize the network.

The first model does not allow the appearance of a network of planar squares, although squares can also fill the plane. In our model this would require the  $Z_4$  symmetry, which is not effective in that model.

The fourth model leads to the model considered in Refs. [21,22]. In this case the three-junction is formed by BPS defects, and we can form an hexagonal array. Here, the three-junction is stable, because each leg carries the same tension. But it does not generate a BPS network, since any two adjacent three-junctions must have different winding to accommodate the three vacuum states in the network, and this would imply that each side of the hexagonal cell must be seen as BPS and anti-BPS, simultaneously, frustrating and destabilizing the network – see Refs. [21–23].

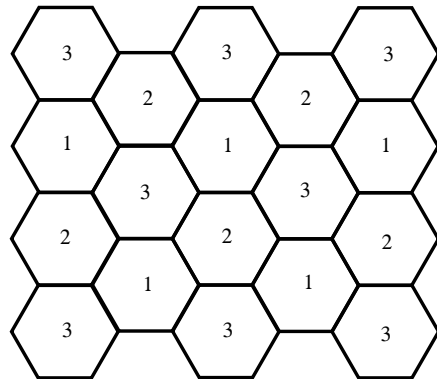


FIG. 6. The regular hexagonal network of non-BPS defects given by the  $Z_3$  model defined by the potential of Eq. (166).

We consider another model, investigated in Ref. [24]. This model is defined by no superpotential, and the argument above is no longer valid. The  $Z_3$  symmetry seems to allow the presence of a network of defects, also in the form of regular hexagonal array. In the thin wall approximation, the hexagonal network that appears in this case is interesting because the solutions are explicitly known, form straight-line segments joining the vacuum states, and have the same energy or tension,  $(9/4)\sqrt{27/8}|\lambda|$ . The  $Z_3$  symmetry that appears in the vacuum sectors is also effective in the sectors of the topological defects. The inequality  $t_{ik} \leq t_{ij} + t_{jk}$  is strictly valid in this case, ensuring stability of the hexagonal network, as depicted in FIG. 6 in the thin wall approximation.

## VII. COMMENTS AND CONCLUSIONS

In the present work we have examined several models of coupled scalar fields. We have found some explicit

solutions, of the BPS and non-BPS type. We have also investigated linear stability, checking the behavior of the bosonic matter on the background of the BPS and non-BPS defects. The BPS states are solutions that obey first-order differential equations, and the non-BPS states are not. The BPS states engender the property of having energy evenly distributed in the gradient and potential portions. However, in the systems of two coupled fields that we have introduced, the non-BPS states also engender the same feature, as we have explicitly shown in this work. The point here is that the non-BPS states of the systems of coupled fields are BPS states of simpler systems, which are projections of systems of coupled fields onto a single, specific field direction.

The first model is the model investigated in Sec. III A. It presents several properties. In particular, it has a rich BPS sector, the sector that connect the minima  $(1,0)$  and  $(-1,0)$  by one-component and two-component BPS states. The two-component state describe a family of solutions, parametrized by the ratio between the coupling constants that specify the system. These one-component and two-component states allow diverse applications, like the applications as bag models in Refs. [27], as defects inside defects in Refs. [11,12,14,15], and in applications to condensed matter, to polymeric chains having two relevant degrees of freedom to represent the chain – see Refs. [4,37].

In applications in the form of bag models, in addition to the models already introduced in Refs. [30,31] we have other possibilities, given by the first, second and third models introduced in Sec. III. These models differ from the model considered in Ref. [41], and we believe that this new direction may shed further light on the issues explored in that work. In particular, it seems that our suggestions are easier to examine, and may offer an analytical understanding of the issues put forward in Ref. [41] under numerical investigations. We recall that the model investigated in [41] is defined by a potential that cannot be reduced to none of the models considered in the present work.

In application to defect inside defect, much work was already done in Refs. [11–15]. The natural extension is now related to issues where one allows the presence of local symmetries, as in the work on superconducting strings [6]. In the first model of Sec III the  $Z_2 \times Z_2$  symmetry can be enlarged by enlarging each one of the two independent symmetries. As we have already commented on in Sec. III, we can for instance make the  $\chi$  field complex, in this case changing the  $Z_2 \times Z_2$  symmetry to  $Z_2 \times U_1(1)$ , if one also includes the Abelian gauge field. This opens new possibilities, providing for instance a natural scenario to the Callan-Harvey effect [40]. Another possibility includes models that presents the  $Z_2 \times Z_3$  symmetry, which may provide scenarios for domain walls that nest planar networks of topological defects. These issues are presently under consideration, and we hope to report on them in the near future.

We have also commented on junctions of defects, and

the subsequent formation of networks of defects. In this case we need to enlarge the spatial dimension from  $d = 1$  to at least the  $d = 2$  case. In the planar case, we have exemplified how to get planar solutions from the unidimensional kinks of the model. Here we have considered three models, the first and the fourth model of Sec. III, and another one, firstly considered in Ref. [24]. These systems are all different: the first model admits a supersymmetric extension of the type  $N = 1$ , and seems to admit no stable network of defects, at least classically; the fourth model presents junctions that break 1/4 supersymmetry, but it also seems to admit no stable network of BPS defects. The other model does not present a supersymmetric extension, but the defect solutions get even contributions from the gradient and potential portions of the energy, and so they behave very much like BPS states. This is crucial for showing that the fusion of defects is a reaction that occurs exothermically, and so the three-junction generates a stable network of defects.

#### Acknowledgments

We thank A.L.L. Guedes, A.S. Inácio, J.R.S. Nascimento, R.F. Ribeiro, and J. Zanelli for discussions. We also thank CAPES, CNPq, and PRONEX for partial support.

- 
- [1] M. K. Prasad and C. M. Sommerfield, Phys. Rev. Lett. **35**, 760 (1975); E. B. Bogomol'nyi, Sov. J. Nucl. Phys. **24**, 449 (1976).
  - [2] D. Bazeia, M.J. dos Santos and R.F. Ribeiro, Phys. Lett. **208A**, 84 (1995).
  - [3] D. Bazeia and M.M. Santos, Phys. Lett. **217A**, 28 (1996).
  - [4] D. Bazeia, R.F. Ribeiro and M.M. Santos, Phys. Rev. E **54**, 2943 (1996).
  - [5] R. Rajaraman, Phys. Rev. Lett. **42**, 200 (1979).
  - [6] E. Witten, Nucl. Phys. B **249**, 557 (1985).
  - [7] G. Lazarides and Q. Shafi, Phys. Lett. B **159**, 261 (1985).
  - [8] R. MacKenzie, Nucl. Phys. B **303**, 149 (1988).
  - [9] J.R. Morris, Phys. Rev. D **51**, 697 (1995).
  - [10] J.R. Morris, Phys. Rev. D **52**, 1096 (1995).
  - [11] D. Bazeia, R.F. Ribeiro, and M.M. Santos, Phys. Rev. D **54**, 1852 (1996).
  - [12] F. A. Brito and D. Bazeia, Phys. Rev. D **56**, 7869 (1997).
  - [13] J.R. Morris, Int. J. Mod. Phys. A **13**, 1115 (1998).
  - [14] J.D. Edelstein, M.L. Trobo, F.A. Brito and D. Bazeia, Phys. Rev. D **57**, 7561 (1998)
  - [15] D. Bazeia, H. Boschi-Filho and F.A. Brito, J. High Energy Phys. **04**, 028 (1999).
  - [16] E. Witten and D. Olive, Phys. Lett. B **78**, 97 (1978).
  - [17] J.A. de Azcárraga, J.P. Gauntlett, J.M. Izquierdo, and P.K. Townsend, Phys. Rev. Lett. **63**, 2443 (1989).
  - [18] G. Dvali and M. Shifman, Phys. Lett. B **396**, 64 (1997).
  - [19] M. Cvetič, F. Quevedo, and S.J. Rey, Phys. Rev. Lett. **67**, 1836 (1991).

- [20] E.R.C. Abraham and P.K. Townsend, Nucl. Phys. B **351**, 313 (1991).
- [21] G.W. Gibbons and P.K. Townsend, Phys. Rev. Lett. **83**, 1727 (1999).
- [22] S.M. Carrol, S. Hellerman, and M. Trodden, *Domain wall junctions are 1/4-BPS states*. hep-th/9905217. Phys. Rev. D. To appear.
- [23] P.M. Saffin, Phys. Rev. Lett. **83**, 4249 (1999).
- [24] D. Bazeia and F.A. Brito, Phys. Rev. Lett. **84**, 1094 (2000).
- [25] H. Oda, K. Ito, M. Naganuma, and N. Sakai, Phys. Lett. B **471**, 140 (1999).
- [26] S.M. Carrol, S. Hellerman, and M. Trodden, *BPS domain wall junctions in infinitely large extra dimensions*. hep-th/9911083.
- [27] J.R. Morris and D. Bazeia, Phys. Rev. D **54**, 5217 (1996). D. Bazeia and J.R. Morris, *Domain walls and nontopological solitons in systems of coupled fields* (unpublished).
- [28] B. Chibisov and M. Shifman, Phys. Rev. D **56**, 7990 (1997); Erratum: Ibid. D **58**, 109901 (1998).
- [29] A. Chodos, R.L. Jaffe, K. Johnson, C.B. Thorn, and V.W. Weisskopf, Phys. Rev. D **9**, 3471 (1974).
- [30] R. Rajaraman and E.J. Weinberg, Phys. Rev. D **11**, 2950 (1975).
- [31] C. Montonen, Nucl. Phys. B **112**, 349 (1976).
- [32] S.M. Carol and M. Trodden, Phys. Rev. D **57**, 5189 (1998).
- [33] A. Campos, K. Holland, and U.-J. Wiese, Phys. Rev. Lett. **81**, 2420 (1998).
- [34] A. Vilenkin and E.P.S. Shellard, *Cosmic strings and other topological defects* (Cambridge UP, Cambridge/UK, 1994).
- [35] A.H. Eschenfelder, *Magnetic bubble technology* (Springer-Verlag, Berlin, 1981).
- [36] D. Walgraef, *Spatio-temporal pattern formation* (Springer-Verlag, New York, 1997).
- [37] D. Bazeia and E. Ventura, Chem. Phys. Lett. **303**, 341 (1999).
- [38] P. Couillet and J. Lega, Phys. Rev. Lett. **65**, 1352 (1990).
- [39] H.M. Ruck, Nucl. Phys. B **167**, 320 (1980).
- [40] G.C. Callan, Jr. and J.A. Harvey, Nucl. Phys. B **250**, 427 (1985).
- [41] P. Peter, J. Phys. A **29**, 5125 (1996).
- [42] S.M. Barr, Phys. Rev. D **55**, 3820 (1997).
- [43] A. Linde, Phys. Rev. D **49**, 748 (1994); J. Garcia-Bellido and A. Linde, Phys. Rev. D **57**, 6075 (1998).
- [44] J.R. Morris, Phys. Rev. D **59**, 023513 (1999).